

Original Contribution

Structure-activity relationship of C6-C3 phenylpropanoids on xanthine oxidase-inhibiting and free radical-scavenging activities

Yuan-Ching Chang^{a,b,1}, Fu-Wei Lee^{c,d,1}, Chien-Shu Chen^e, Sheng-Tung Huang^f, Shin-Hui Tsai^c,
Shih-Hao Huang^g, Chun-Mao Lin^{c,d,*}

^a Department of General Surgery, Mackay Memorial Hospital, Taipei, Taiwan

^b Mackay Medicine, Nursing and Management College, Beitou, Taipei, Taiwan

^c Graduate Institute of Medical Sciences, Taipei Medical University, Taipei, Taiwan

^d Topnotch Stroke Research Center, Taipei Medical University, Taipei, Taiwan

^e School of Pharmacy, College of Medicine, National Taiwan University, Taipei, Taiwan

^f Institute of Biotechnology, National Taipei University of Technology, Taipei, Taiwan

^g Department of Food Science, Taipei College of Maritime Technology, Taipei, Taiwan

Received 13 April 2007; revised 9 August 2007; accepted 17 August 2007

Available online 4 September 2007

Abstract

We employed the techniques of DNA relaxation, DPPH (1,1-diphenyl-2-picrylhydrazyl hydrate), and DMPO (5,5-dimethyl-1-pyrroline-*N*-oxide)-electron spin resonance (ESR), to study the effects of reactive oxygen species (ROS) suppression by 11 selected C6-C3 phenylpropanoid derivatives under oxidative conditions. We also investigated the effects of the derivatives on the inhibition of xanthine oxidase (XO) activity, and the structure-activity relationships (SARs) of these derivatives against XO activity were further examined using computer-aided molecular modeling. Caffeic acid was the most potent radical scavenger among the 11 test compounds. Our results suggest that the chemical structure and number of hydroxyl groups on the benzene ring of phenylpropanoids are correlated with the effects of ROS suppression. All test derivatives were competitive inhibitors of XO. The results of the structure-based molecular modeling exhibited interactions between phenylpropanoid derivatives and the molybdopterin region of XO. The *para*-hydroxyl of phenylpropanoid derivatives was pointed toward the guanidinium group of Arg 880. The phenylpropanoid derivatives containing the *meta*- or *ortho*-hydroxyl formed hydrogen bonds with Thr 1010. In addition, *meta*-hydroxyl formed hydrogen bonds with the peptide bond between the residues of Thr1010 and Phe1009. CAPE, the phenylethyl ester of phenylpropanoids, had the highest affinity toward the binding site of XO, and we speculated that this was due to hydrophobic interactions of the phenylethyl ester with several hydrophobic residues surrounding the active site. The hypoxanthine/XO reaction in the DMPO-ESR technique was used to correlate the effects of these phenylpropanoid derivatives on enzyme inhibition and ROS suppression, and the results showed that caffeic acid and CAPE were the two most potent agents among the tested compounds. We further assessed the effects of the test compounds on living cells, and CAPE was the most potent agent for protecting cells against ROS-mediated damage among the tested phenylpropanoids.

© 2007 Elsevier Inc. All rights reserved.

Keywords: Caffeic acid; CAPE; Molecular modeling; Phenylpropanoid; ROS; Xanthine oxidase

Abbreviations: CAPE, caffeic acid phenethyl ester; DHR123, dihydrorhodamine 123; DMEM, Dulbecco's modified Eagle's medium; DMPO, 5,5-dimethyl-1-pyrroline-*N*-oxide; DPPH, 1,1-diphenyl-2-picrylhydrazyl hydrate; FBS, fetal bovine serum; LPS, lipopolysaccharide; MEM, minimum essential medium; ROS, reactive oxygen species; SARs, structure-activity relationships; XDH, xanthine dehydrogenase; XO, xanthine oxidase; XPH, hypoxanthine.

* Corresponding author. College of Medicine, Taipei Medical University, 250 Wu-Hsing Street, Taipei 110, Taiwan. Fax: +886 2 27387348.

E-mail address: cmlin@tmu.edu.tw (C.-M. Lin).

¹ Contributed equally to this work.

Introduction

Oxidative stress has been implicated in an enormous variety of physiological and pathological processes. An oxidation-reduction imbalance in a healthy living system leads to malfunctioning of cells that can ultimately result in various

diseases, including aging, cancer, neurological degeneration, and arthritis. The toxicity ascribed to the superoxide radical is believed to be caused by superoxide's direct interaction with biological targets. Reactive oxygen species (ROS) can initiate a wide range of toxic oxidative reactions [1]. ROS released by phagocytic cells are involved in the link between inflammation and cancer. Excessive and persistent formation of ROS by inflammatory cells is thought to be a key factor in genotoxic effects.

Xanthine oxidase (XO) is an important source of free radicals and has been reported in various physiological and pathological models. XO causes gout and is responsible for oxidative damage to living tissues. This enzyme reduces molecular oxygen, leading to the formation of $O_2^{\cdot-}$ and hydrogen peroxide. Regulation of XO activity is important during inflammation [2]. XO is a secreted enzyme which is formed in the liver as xanthine dehydrogenase (XDH) and binds to the vascular endothelium. High expression of XDH is found in the liver, and it is converted to the radical-forming XO on atherosclerosis development in mice. Treatment with an XO inhibitor largely prevents the development of endothelial dysfunction and atherosclerosis in mice [3]. XO catalyzes the oxidation of hypoxanthine and xanthine to uric acid yielding superoxide radicals and raises the oxidative level in an organism. Hydroxylation takes place at the molybdopterin center (Mo-pt) via a Mo-OH oxygen forming a bond with a carbon atom of the substrate such that the oxygen atom is derived from water rather than molecular oxygen [4]. The active form of XO is a homodimer with a molecular weight of 290 kDa with each of the monomers acting independently during catalysis. Each subunit contains one molybdopterin cofactor, two distinct [2Fe-2S] centers, and one FAD cofactor [5]. The cocrystalline structure of salicylate-XO was first reported by Enroth et al. [6]. Several amino acid residues, including Arg 880, Phe 914, Phe 1009, Thr 1010, and Glu 1261, are important for salicylate binding via hydrogen and electrostatic interactions. Although salicylate itself does not bind to the Mo-pt cofactor, it blocks the approach of substrates toward the metal complex.

Natural polyphenols can be divided into several different classes depending on each one's basic chemical structure, which ranges from simple molecules to highly polymerized compounds. Phenylpropanoid derivatives (C6-C3) are an important group of low-molecular-weight phenolics [7]. The most important phenylpropanoids are the hydroxycinnamic acids and their derivatives. Phenylpropanoid inhibition of XO has been reported. Structure-activity relationships (SARs) of caffeic acid analogues interacting with this enzyme have also been discussed [8]. However, the influence of enzyme-substrate binding by phenylpropanoids and the stereochemistry with XO have not been characterized. In this study, the protective effects of some C6-C3 phenylpropanoids against ROS and their influence on binding to the active site of XO according to various substitution groups and positions on phenylpropanoids were investigated. We also combined the role of ROS scavenging and XO inhibition of phenylpropanoids in order

to identify which compounds are more vital for therapeutic applications.

Materials and methods

Materials

Xanthine oxidase (EC 1.2.3.2.), xanthine, allopurinol, cinnamic acid [(E)-3-phenyl-2-propenoic acid], caffeic acid, ferulic acid, isoferulic acid, *p*-hydroxycinnamic acid (*p*-coumaric acid), *o*-coumaric acid, *m*-coumaric acid, *p*-methoxycinnamic acid, *o*-methoxycinnamic acid, *m*-methoxycinnamic acid, caffeic acid phenethyl ester (CAPE), and lipopolysaccharide (LPS) (*Escherichia coli* O127:B8) were purchased from Sigma (St. Louis, MO) (Table 1). All of the solvents used in this study were from E. Merck (Darmstadt, Germany). Dulbecco's modified Eagle's medium (DMEM) and minimum essential medium (MEM), fetal bovine serum (FBS), penicillin, and streptomycin were obtained from Gibco BRL (Grand Island, NY). β -Amyloid peptide (A β_{25-35} fragment) was purchased from Jerini Peptide Technologies (Berlin, Germany).

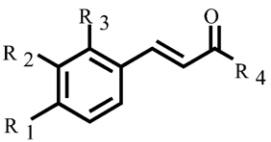
Cell culture

The mouse monocyte-macrophage cell line, RAW 264.7 (ATCC TIB-71; American Type Culture Collection, Manassas, VA), was cultured in DMEM supplemented with 10% heat-inactivated FBS. Cells were plated at a density of 1.0×10^6 /ml for 18–24 h before activation by LPS (50 ng/ml). Neuro 2A neuroblastoma cells (BCRC 60026) were purchased from CCRC (Culture Collection and Research Center, Hsinchu, Taiwan). Cells were grown in MEM containing 10% FBS, 1% nonessential amino acid, and 100 μ g/ml penicillin-streptomycin. Conditions were maintained in a humidified 95% air/5% CO₂ incubator at 37°C.

Supercoiled DNA-relaxation assay

The inhibitory effect of phenylpropanoids on supercoiled DNA strand breakage caused by the Fenton reaction was evaluated [9]. pUC-19 plasmid DNA (200 ng) was incubated at 37°C for 30 min in TE buffer (10 mM Tris and 1 mM EDTA; pH 8.0) containing 100 mM H₂O₂ and 50 μ M ferrous sulfate in the presence or absence of 5.0 μ M flavonoids in a final volume of 20 μ l. The conversion of the covalently closed circular double-stranded supercoiled DNA to a relaxed open-circle form was used to evaluate DNA strand breakage induced by the Fenton reaction. DNA strand breaks induced by the Fenton reaction occurred rapidly, with most of the supercoiled pUC-19 NDA converted to the relaxed form after a 30-min incubation at 37°C. Then, the samples were loaded onto a 1% agarose gel, and electrophoresis was performed in a TAE buffer (40 mM Tris-acetate and 1 mM EDTA) in the presence of 0.5 μ g/ml of ethidium bromide. After electrophoresis, the gel was photographed under transmitted ultraviolet light.

Table 1
Chemical structures of various phenylpropanoid derivatives

Chemical formula	Name	Substitution			
		R1	R2	R3	R4
	trans-cinnamic acid	H	H	H	OH
	p-coumaric acid	OH	H	H	OH
	p-methoxycinnamic acid	OCH ₃	H	H	OH
	m-coumaric acid	H	OH	H	OH
	m-methoxycinnamic acid	H	OCH ₃	H	OH
	o-coumaric acid	H	H	OH	OH
	o-methoxycinnamic acid	H	H	OCH ₃	OH
	caffeic acid	OH	OH	H	OH
	ferulic acid	OH	OCH ₃	H	OH
	isoferulic acid	H	OH	H	OH
	CAPE (caffeic acid phenethyl ester)	OH	OH	H	O-phenethyl ring

DPPH (1,1-diphenyl-2-picrylhydrazyl hydrate) radical-scavenging assay

The reaction was performed in 3 ml of methanol containing 250 μ M of freshly prepared DPPH. The reaction mixtures were protected from light and incubated for 90 min at room temperature, after which the absorbance of the remaining DPPH was determined colorimetrically at 517 nm. The scavenging activities of the phenylpropanoids were measured as the decrease in absorbance of DPPH expressed as a percentage of the absorbance of a control DPPH solution without phenylpropanoids [10].

XO activity assay

The enzyme activity of XO was measured spectrophotometrically by continuously measuring uric acid formation at 295 nm with xanthine as the substrate. The XO assay consisted of a 500- μ l reaction mixture containing 7.5 mM phosphate buffer, 20 mM 3-(cyclohexylamino)-1-propanesulfonic acid (CAPS), 38 μ M EDTA (pH 7.0), 3 U xanthine oxidase, and 10–60 μ M xanthine as the substrate. The assay was initiated by adding the enzyme to the reaction mixture with or without inhibitors. The assay mixture was incubated for 3 min at 37°C, and absorbency readings were taken every 5 s [11]. The substrate concentration was kept to less than 60 μ M to avoid substrate inhibition. All data obtained from the enzyme kinetic assays and plotting were processed using Excel (Microsoft Office 2003, Microsoft Taiwan).

Computational molecular docking

To explore the probable binding interactions of the inhibitors with XO, we performed molecular modeling studies using the docking program, AutoDock (version 3.0) [12]. AutoDock can dock conformationally flexible ligands into a protein, while keeping the protein fixed. The X-ray crystalline structure of bovine XO in complex with salicylate (PDB ID code 1FIQ, Protein Data Bank: <http://www.rcsb.org/pdb>) [6] was used for the docking studies. The A- and B-chains of protein and all small

molecules were removed except the two structural waters, Wat176 and Wat196, at the active site. The Wat176 water molecule was found to be H-bonded to the carboxylate group of salicylate. In addition, an oxygen atom single-bonded to the Mo ion was replaced with a water molecule to mimic the water supply during enzyme catalysis. After the addition of polar hydrogens, the protein atoms were assigned Kollman united-atom partial charges. The 3D structures of the inhibitor molecules were built and optimized by energy minimization using the Tripos force field in the software package, SYBYL 6.5 (Tripos, St. Louis, MO). The partial atomic charges were calculated using the Gasteiger-Marsili method [13]. The rotatable bonds in the ligands were assigned with AutoTors implemented in the AutoDock program. To carry out docking simulations, a grid box was defined to enclose the active site with dimensions of 22.5 \times 22.5 \times 22.5 Å and a grid spacing of 0.375 Å. The grid maps for energy scoring were calculated using AutoGrid. Docking calculations were performed using the Lamarckian genetic algorithm (LGA) and the pseudo-Solis and Wets local search method. Default parameters were used except for the maximum number of energy evaluations (1×10^6) and docking runs (100). From the docking results, the best-scoring (i.e., the lowest docking energy) docked model of a compound was chosen to represent its most favorable binding mode predicted by AutoDock. In the present study, all computer simulations were performed on a Silicon Graphics Octane workstation (R12000 with a 270-MHz dual processor) or a Silicon Graphics O2 workstation (R5000 with a 180-MHz single processor).

Electron spin resonance (ESR)-trapping assay

Inhibition of iron-induced \cdot OH formation was determined using the ESR-trapping technique in combination with DMPO (5,5-dimethyl-1-pyrroline-N-oxide). The DMPO-OH adduct was obtained from the Fenton reaction system containing 60 mM DMPO, 2 mM H₂O₂, and 50 μ M ferrous ammonium sulfate with or without the test sample. This mixture was transferred to a flat quartz cell, and the ESR spectrum was measured 40 s after the addition of ferrous ammonium sulfate.

The spin adducts generated in the reaction system were detected using a Bruker ER070 spectrometer (Karlsruhe, Germany) at room temperature [14]. Instrumental conditions were as follows: a central magnetic field of 3475 G, an X-band modulation frequency of 100 kHz, power of 6.4 mW, a modulation amplitude of 5 G, a time constant of 655.4 ms, and a sweep time of 83.9 s. The ESR spectra were measured at room temperature. The intensity of the DMPO-OH spin adduct was evaluated by comparing the peak height of the DMPO-OH signal.

Combined ROS scavenging and XO inhibition activities were measured using the DMPO spin adduct generated in the hypoxanthine (HPX) and XO reaction system by the spin-trapping method [15]. Specifically, 20 μ l of a sample solution was mixed with 30 μ l of 5 mM HPX, after which 20 μ l of 5.5 mM diethylenetriaminepentaacetic acid (DTPA), 10 μ l of 9 M DMPO, and 20 μ l of 0.4 U/ml XO solution were added to the reaction solution in a test tube. The measurement was taken immediately after the mixture was quickly stirred. A 200- μ l aliquot of the mixture was placed into a flat cell.

Determination of nitrite

The nitrite accumulating in the culture medium was measured as an indicator of NO production according to the Griess reaction. Cells were plated in 24-well culture plates and stimulated with LPS (100 ng/ml) in the presence or absence of test phenylpropanoids for 24 h. An aliquot of 100 μ l of the culture medium (cell free) was mixed with 50 μ l of 1% sulfanilamide (in 5% phosphoric acid) and 50 μ l of 0.1% naphthylethylenediamine dihydrochloride at room temperature. The absorbance at 550 nm was measured with a sodium nitrite serial dilution standard curve, and nitrite production was determined [16].

Measurements of intracellular ROS

Levels of cellular oxidative stress were measured using the fluorescent probe, dihydrorhodamine 123 (DHR123), as described previously [17]. The DHR123 dye enters mitochondria and fluoresces when oxidized by ROS. After treatment with 100 μ M LPS or cotreatment with CAPE (1 μ M), caffeic acid (10 μ M), or allopurinol (10 μ M), respectively, and LPS for 1 h, cells were stained with 10 μ M DHR123 for 30 min and washed with phosphate-buffered saline. Cells were imaged using a confocal microscope (Leica TCS SP5, Bensheim, Germany). Cells were located under bright-field optics and then scanned once with a laser (with excitation at 488 nm and emission at 510 nm).

Flow cytometric detection of intracellular ROS was performed as described previously [18]. RAW 264.7 cells were suspended in phenol red-free media at a concentration of 2×10^5 cells/ml. Cells were stained with 100 μ M 2',7'-dichlorofluorescein diacetate (DCF-DA) in the dark for 30 min and then analyzed using FACScan (Becton Dickinson, Franklin Lakes, NJ). Oxidation of the green DCF fluorescence in living cells was detected using the FL1-H wavelength band. The

fluorescence signals of 10,000 cells were processed using a logarithmic amplifier.

Statistical analysis

The results are represented as the mean \pm standard deviation from three independent experiments ($n=3$). Statistical analysis was performed using analysis of variance (ANOVA).

Results

The inhibitory effects on DNA relaxation activities, 1,1-diphenyl-2-picrylhydrazyl, and DMPO-OH by various test compounds were assessed for their antioxidant activities. Hydroxyl radicals (\cdot OH) generated by the Fenton reaction are known to cause oxidative-induced DNA strand breakage which yields relaxed, circular DNA. The hydroxyl radical-scavenger properties of the test compounds on reducing the supercoiled DNA strand breakage caused by hydroxyl radicals were evaluated. Fig. 1A shows the results obtained from an agarose gel of pUC-19 plasmid DNA that was subjected to the Fenton reaction in the presence or absence of the test compounds. DNA strand breakage could be induced *in vitro* in the presence of H_2O_2 and Fe^{2+} (lane 3). These results showed that caffeic acid and CAPE were more effective in reducing DNA relaxation than the other phenylpropanoids tested. Ferulic acid, isoferulic acid, and coumaric acids had comparable antioxidative activities. Methoxycinnamic acids and cinnamic acid showed no antioxidative activities in this assay system.

DPPH radicals have been used as another method for evaluating the antioxidant activities of antioxidative agents. We also evaluated the antioxidative activities of the test compounds under DPPH radical conditions, and the results are shown in Table 2. Once again, caffeic acid and CAPE were the two most potent agents in reducing DPPH radicals (83.59 and 73.93% inhibition, respectively, as compared to ascorbic acid with 76.52% inhibition) among the phenylpropanoids tested. Ferulic acid displayed a less-potent effect with 59.16% inhibition. Methoxycinnamic acids and cinnamic acid exhibited comparable effects in scavenging DPPH radicals.

ESR in combination with the spin-trapping techniques was utilized to further verify that the test compounds examined herein possess the ability to scavenge hydroxyl radicals, and the results are shown in Fig. 1B. 5-Dimethyl-1-pyrroline-*N*-oxide is a spin-trapping reagent that reacts with hydroxyl radicals to generate the spin resonance signal, and this spin resonance signal can be quantified with ESR. The hydroxyl radical scavenger competes with DMPO for hydroxyl radicals; thus diminishing the electron spin resonance signal. In the absence of an antioxidant, 2 mM H_2O_2 and 50 μ M $FeSO_4$ generate an electron spin resonance signal with a peak height of 96; but under the same conditions, the peak heights of ESR signals were reduced to 10 in the presence of 200 μ M caffeic acid (Fig. 1B, left panel). The IC_{50} value of caffeic acid was 65.44 μ M, while that of CAPE was 156.71 μ M (Fig. 1B, right panel). The results were combined with prior results of the DNA protection and DPPH radical experiments, which suggested that caffeic acid

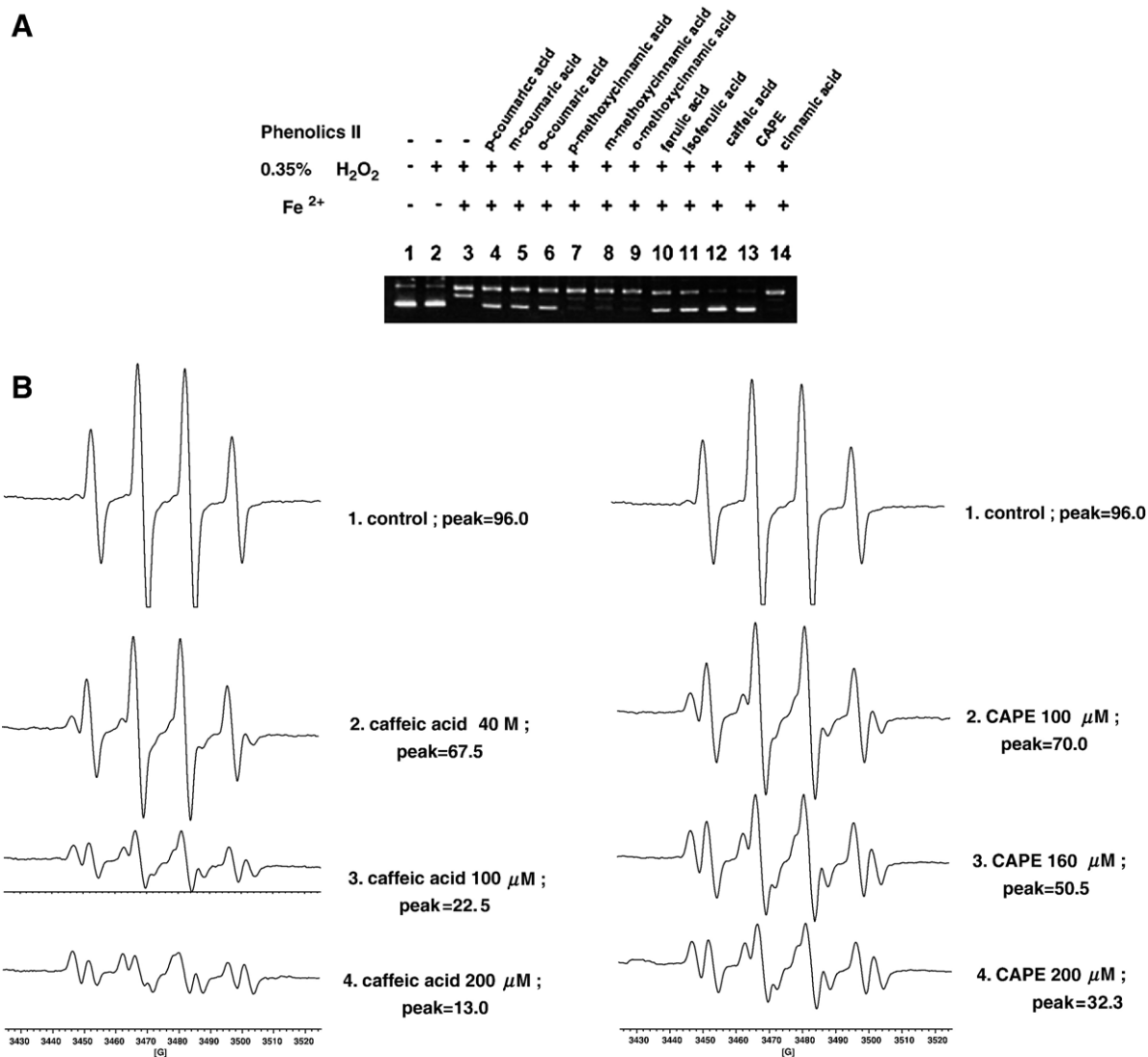


Fig. 1. Antioxidative activities of C6-C3 phenylpropanoid derivatives on intact DNA and in the electron spin resonance (ESR) spectrum. (A) pUC-19 plasmid DNA subjected to the Fenton reaction in the absence (lanes 1–3) or presence of phenylpropanoids (lanes 4–14). pUC-19 plasmid DNA was incubated at 37°C for 30 min with 0.35% H₂O₂ and 50 μM ferrous sulfate in the absence or presence of 50 μM of the test compounds. (B) Effects of caffeic acid and CAPE on DMPO-OH formation. ESR spectra of the DMPO-OH adduct were obtained from the Fenton reaction system with caffeic acid (left panel) and CAPE (right panel) at various concentrations. Reaction mixtures contained 60 mM DMPO, 50 μM Fe(II), and 2 mM H₂O₂ (control) or various concentrations of the respective test compounds.

and CAPE are the two most effective radical scavengers among the tested phenylpropanoids.

Competitive inhibition of XO by phenylpropanoids

The xanthine/xanthine oxidase (X/XO) reaction is an important biological source of ROS generation, and this reaction is known to be involved in many pathological processes. An inhibitor of XO has the potential to be a therapeutic agent for hyperuricemia and ROS-induced diseases. Allopurinol, a potent inhibitor of XO, is clinically used for treating gout to prevent urate from accumulating in joints. XO has been reported to be inhibited by cinnamic acid derivatives. Since the compounds tested herein are structural analogues of cinnamic acid, we were also interested in studying the effects of

these compounds on the activities of XO. Thus, we assayed the test compounds with XO in the presence of X, and the results were analyzed by Lineweaver-Burk plots. The Lineweaver-Burk plot revealed that CAPE competitively inhibited XO (Fig. 2) with an IC₅₀ of 6.26 μM compared to an IC₅₀ of 1.47 μM for allopurinol (Table 3). The IC₅₀ values of selected compounds are listed in Table 3. Caffeic acid, ferulic acid, isoferulic acid, *p*-coumaric acid, and *p*-methoxycinnamic acid were also competitive inhibitors with IC₅₀ values of 65.58, 93.88, 143.19, 96.85, and 183.96 μM, respectively. In contrast, *o*- and *m*-coumaric acids, *o*- and *m*-methoxycinnamic acids, and cinnamic acid showed no significant inhibitory activities (IC₅₀ values of >200 μM) in this assay. CAPE was the most potent inhibitor against XO among the tested compounds. These results indicated that all selected cinnamic acid analogues were

Table 2
Scavenging effects on stable DPPH radicals by phenylpropanoid derivatives

Compound	DPPH inhibition (%)
Ascorbic acid	76.52±3.99
Caffeic acid	83.59±2.94
CAPE	73.93±3.24
Ferulic acid	59.16±3.60
Isoferulic acid	14.09±2.82
<i>p</i> -Coumaric acid	10.40±5.44
<i>m</i> -Coumaric acid	14.96±7.88
<i>o</i> -Coumaric acid	10.63±6.35
<i>p</i> -Methoxycinnamic acid	14.55±6.67
<i>m</i> -Methoxycinnamic acid	14.639±3.89
<i>o</i> -Methoxycinnamic acid	12.39±6.10
<i>di</i> -Methoxycinnamic acid	13.68±4.15
<i>trans</i> -Cinnamic acid	15.52±8.15

The percentage (%) inhibition was calculated according to the formula: [(value of the control – value of phenylpropanoid)/(value of the control)] × 100%.

competitive inhibitors of XO; therefore, they inhibited XO activities through a substrate binding blockade.

3D modeling the docking of phenylpropanoids on XO

Numerous scientists have investigated the inhibitory effects of cinnamic acid analogues on XO, and attempts have been made to elucidate the SARs. We were also interested in visualizing the effects of the tested phenylpropanoids on XO in order to gain insights into the observed activities; a 3D molecular model was created to evaluate the docking of selected compounds on XO. From prior kinetic assays, we learned that the test compounds were competitive inhibitors; therefore, we focused on phenylpropanoid dockings on the active site, the molybdopterin domain of XO. Caffeic acid binds to the molybdopterin domain of XO, which forms several hydrogen bonds with the protein residues. The O atom of the R1-hydroxyl of caffeic acid closely interacts with the guanidinium group of Arg 880. The H atom of the R2-hydroxyl of caffeic acid forms H bonds with the hydroxyl side chain of Thr 1010, and the O atom of the R2-hydroxyl of caffeic acid also forms a hydrogen bond with the H atom of the

Table 3
Fifty percent inhibitory concentrations (IC₅₀) of xanthine oxidase by phenylpropanoid derivatives

Compound	IC ₅₀ (μM)
Allopurinol	1.47±0.32
Caffeic acid	65.58±2.71
CAPE	6.26±1.60
Ferulic acid	93.88±18.95
Isoferulic acid	143.19±2.60
<i>p</i> -Coumaric acid	96.85±3.55
<i>m</i> -Coumaric acid	>200
<i>o</i> -Coumaric acid	>200
<i>p</i> -Methoxycinnamic acid	>200
<i>m</i> -Methoxycinnamic acid	183.96±1.24
<i>o</i> -Methoxycinnamic acid	>200
<i>di</i> -Methoxycinnamic acid	>200
<i>trans</i> -Cinnamic acid	>200

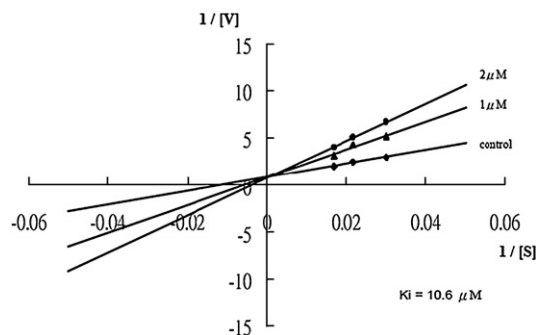


Fig. 2. Kinetic assays of xanthine oxidase inhibition by CAPE. A Lineweaver-Burk double-reciprocal plot was constructed for the inhibition of xanthine oxidase by CAPE. The plot is expressed as 1/velocity vs 1/xanthine (μM^{-1}) without or with an inhibitor in the reaction solution.

peptide bond between F 1009 and Thr 1010. Finally, the carbonyl part of caffeic acid forms hydrogen bonds with the H atom of Ser 876 (Fig. 3A). CAPE is a phenethyl ester of caffeic acid which also exhibits potent affinity toward the molybdopterin domain of XO. On CAPE's docking with the molybdopterin domain of XO, the results revealed that the phenethyl group of CAPE stretched to the space surrounding several hydrophobic residues including Phe 1076, Phe 649, Leu 648, Leu 873, and Leu 1014. The phenyl side chain of the amino acid residues, Phe 1009 and Phe 1076, was oriented perpendicular facing the two aromatic rings of CAPE, which established hydrophobic stabilizing forces (D). Although ferulic acid (B) and *p*-coumaric acid (C) exhibited less affinity toward XO compared to caffeic acid from the enzyme kinetic assays, both compounds also docked at the Mo-pt center in the same orientation as caffeic acid according to results of the molecular docking experiment. One major difference was that ferulic acid and *p*-coumaric acid positioned themselves in a overturned arrangement as caffeic acid binding; this resulted in Ser 876 being separated from the carbonyl, reducing the hydrogen bonding to Arg 880. Cinnamic acid lacks a hydroxyl group, and when connected to the benzene ring, displayed a very low affinity toward the enzyme (Suppl. Fig. 1). Even though these results are not firm evidence as with X-ray crystallography, the docking interactive energies of the various test compounds (Suppl. Table 1) reflect their affinities and are consistent with the IC₅₀ values.

Total activities of reducing ROS formation and ROS scavenging by phenylpropanoids in the hypoxanthine/XO reaction

In addition to possessing ROS scavenging activity, phenylpropanoids also inhibit XO activity leading to a reduction in ROS formation. From prior experimental results, CAPE was the most potent inhibitor of XO among the tested compounds, and caffeic acid was the most effective agent at ROS scavenging. We used ESR combined with the DMPO-trapping assay with xanthine/hypoxanthine in the presence or absence of phenylpropanoids to evaluate their total activities for ROS scavenging and reducing ROS formation, and the results are

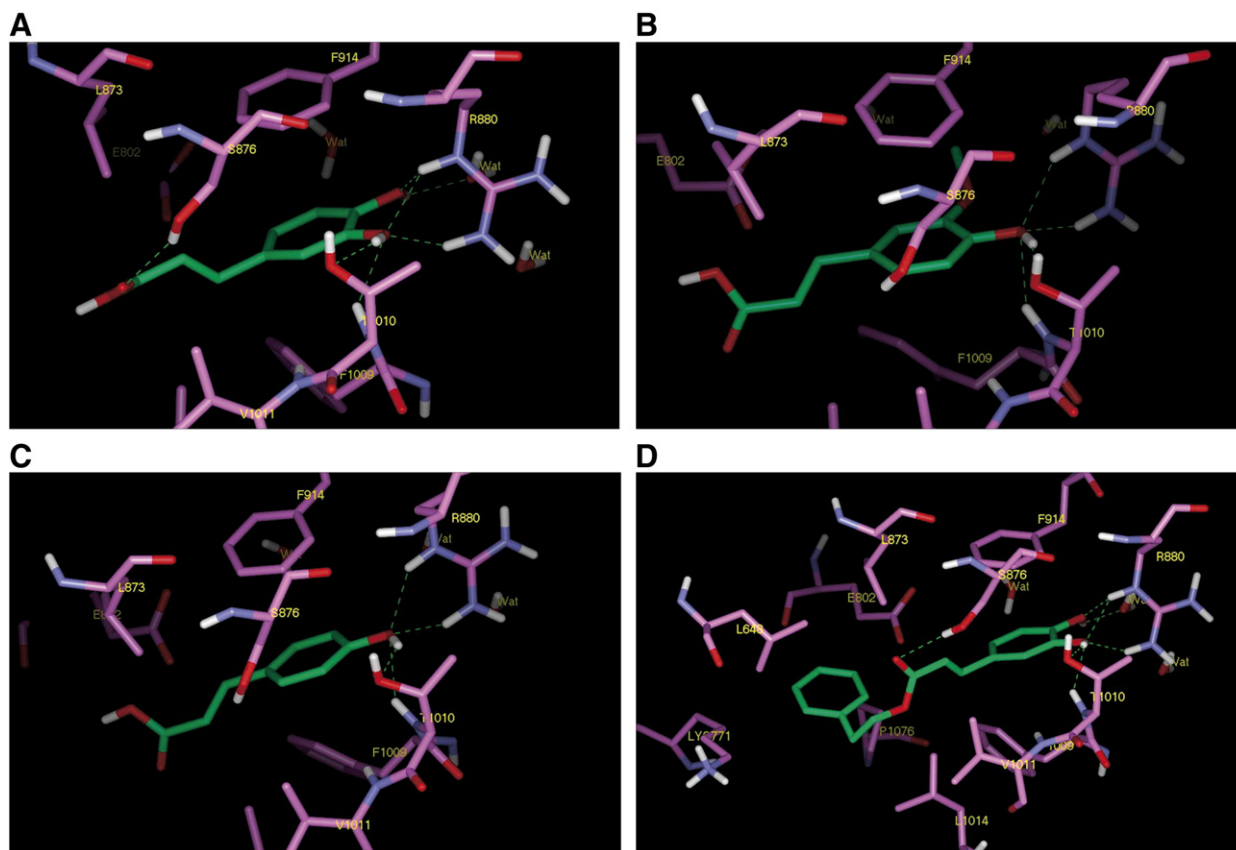


Fig. 3. Molecular model of phenylpropanoid binding to the active site of xanthine oxidase. A three-dimensional model of phenylpropanoid derivatives: (A) caffeic acid, (B) ferulic acid, (C) *p*-coumaric acid, and (D) caffeic acid phenethyl ester.

shown in Table 4. Caffeic acid (82.44% inhibition) was the most potent agent competing with DMPO for ESR signals compared to CAPE (79.51% inhibition). Supplemental Fig. 2 shows the dose-dependent manner of the suppression of the ESR peak heights with caffeic acid and CAPE treatments. Ferulic acid displayed a weaker effect, whereas coumaric acids,

methoxycinnamic acids, and cinnamic acid exhibited substantially weaker effects.

Phenylpropanoids inhibited ROS-associated NO production in living cells

ROS have been viewed as general messengers for signaling pathways which are associated with key biochemical events during inflammation. It has been reported that suppression of ROS-mediated NO elevation is beneficial in reducing the development of inflammation. Nitrite production was used as an indicator of NO release in LPS-activated macrophages. Nitrite concentrations in culture media were measured with and without phenylpropanoid derivatives of coincubated macrophages activated by LPS (100 ng/ml). When LPS was administered to RAW 264.7 macrophages, NO production dramatically increased. The inhibition of NO released with respect to the control LPS-activated macrophages coincubated with the tested phenylpropanoids and relative reference compounds respectively is shown in Table 5. The IC₅₀ values of CAPE, caffeic acid, allopurinol, ascorbic acid, and the nitric oxidase synthase inhibitor, aminoguanidine, were 3.6, 45.5, 55.2, 44.0, and 24.0 μM, respectively; these were calculated from the various concentrations with inhibitory effects on NO production. CAPE was the most potent NO-suppressive agents in LPS-treated macrophages.

Table 4

Total activities of reduced reactive oxygen species (ROS) formation and ROS scavenging by phenylpropanoids in the hypoxanthine/xanthine oxidase reaction using electron spin resonance (ESR) combined with the DMPO-trapping assay

Compound	DMPO–OOH inhibition (%)
Allopurinol	30.82±2.98
Caffeic acid	82.44±1.57
CAPE	79.91±8.75
Ferulic acid	25.86±3.61
Isoferulic acid	23.23±4.07
<i>p</i> -Coumaric acid	23.81±5.56
<i>m</i> -Coumaric acid	10.48±5.36
<i>o</i> -Coumaric acid	17.83±5.36
<i>p</i> -Methoxycinnamic acid	12.55±3.01
<i>m</i> -Methoxycinnamic acid	11.59±2.44
<i>o</i> -Methoxycinnamic acid	11.28±4.99
<i>di</i> -Methoxycinnamic acid	11.42±3.84
<i>trans</i> -Cinnamic acid	9.16±3.86

The percentage (%) inhibition was calculated according to the formula: [(peak height of the control – peak height of phenylpropanoid)/(peak height of the control)] × 100%.

Table 5
Inhibition of NO production in lipopolysaccharide (LPS)-activated macrophage cells

Compound	Concentration (μM)	Inhibition (%) ^a
CAPE	1	2.31 \pm 5.07
	2	24.34 \pm 2.49
	4	55.01 \pm 2.96
Caffeic acid	10	19.16 \pm 7.79
	20	24.77 \pm 0.90
	40	42.81 \pm 5.31
Cinnamic acid	10	0.00 \pm 0.00
	20	18.38 \pm 8.59
	40	40.17 \pm 2.70
Allopurinol	10	14.49 \pm 2.73
	20	27.28 \pm 4.43
	40	36.65 \pm 3.83
Aminoguanidine	10	40.45 \pm 12.63
	20	59.66 \pm 8.43
	40	78.62 \pm 2.51
Ascorbate	10	9.49 \pm 0.96
	20	27.11 \pm 12.56
	40	43.51 \pm 1.36

^a Percentage inhibition of NO production was determined as the accumulated nitrite concentration in medium with the Griess reagent 20 h after stimulation by LPS (100 ng/ml). Data are presented as the mean \pm SD of three experiments.

In an attempt to identify phenylpropanoid inhibition of ROS-associated NO production, cells were incubated with DHR123. This nonfluorescent compound selectively accumulates in mitochondria, where it is oxidized by mitochondria-derived ROS to a fluorescent rhodamine derivative. As demonstrated in Fig. 4A, LPS treatment (b) resulted in a significant increase in DHR123 fluorescence compared to the untreated control (a), while a reduced fluorescence intensity was seen with LPS and CAPE cotreatment (c). Caffeic acid (d) and allopurinol (e) displayed weaker suppressive activities on the fluorescence

intensity than CAPE. These results show that CAPE was more effective in reducing an LPS-induced rise in ROS levels. This is consistent with the notion that CAPE is the most potent NO-suppressive agent in LPS-treated macrophages. Flow cytometric detection of intracellular ROS (Fig. 4B) was performed by examining the oxidation of green DCH fluorescence in RAW 264.7 cells. Phenylpropanoid inhibition of ROS-associated green DCH fluorescence on LPS treatment (100 ng/ml) for 60 min was consistent with the results of DHR123 staining, in that CAPE (b) was more effective in reducing the LPS-induced rise in the DCH fluorescence intensity. The order of the inhibition effects was CAPE > *p*-hydroxycinnamic acid > allopurinol > cinnamic acid.

Discussion

Our study demonstrates that selected phenylpropanoids are competitive inhibitors against XO, and they are also potent superoxide-suppressive agents. Hydroxycinnamic acids, coumaric acid, ferulic acid, and caffeic acid are abundant in various plant extracts. The concentrations of these compounds have been used as an index of the effectiveness of the extraction process. Caffeic acid has been shown to be the most effective in scavenging ROS [19–21]. CAPE, the active ingredient in honeybee propolis, has been determined to have antioxidant, anti-inflammatory, antiviral, and anticancer activities. In various in vivo experiments, rats with ameliorated clinical symptoms treated with CAPE showed a significant reduction in ROS production [22]. Our results in Fig. 1 demonstrate that the chemical structures of both caffeic acid and CAPE bear two hydroxyl moieties on the benzene rings, and these were the two most effective radical scavengers among the tested compounds. All other selected phenylpropanoids only carried one hydroxyl

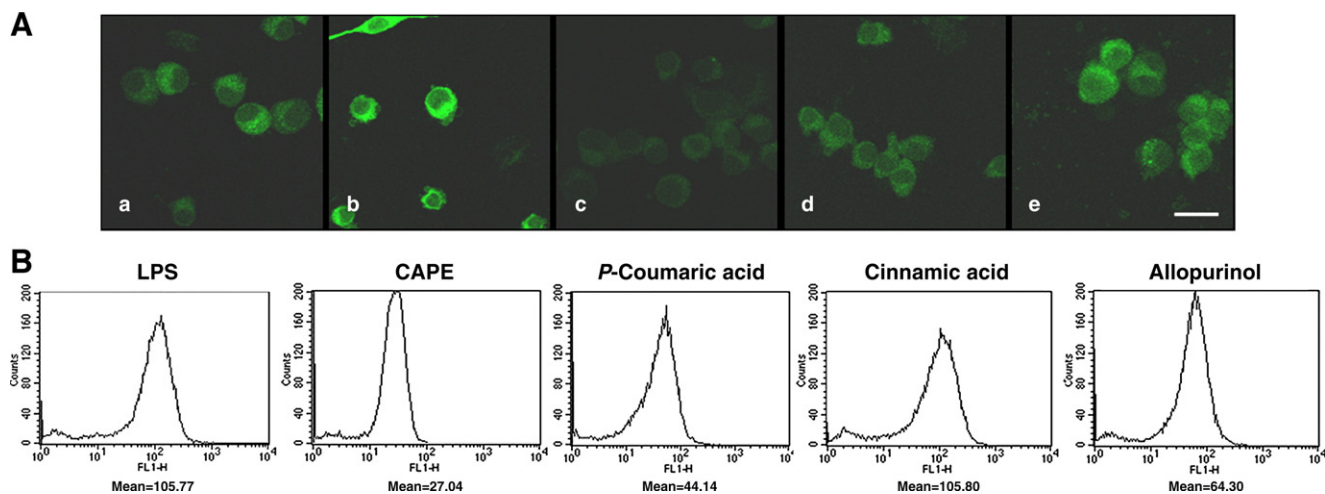


Fig. 4. Reduction of reactive oxygen species (ROS) amounts in LPS-activated macrophage cells by C6–C3 phenylpropanoids. (A) ROS amounts in LPS-treated RAW 264.7 cells as measured by DHR123 fluorescence of the (a) control, (b) 1 h following 100 ng/ml LPS addition, (c) 1 h following 100 ng/ml LPS with CAPE addition (1 μM), (d) 1 h following 100 ng/ml LPS with caffeic acid addition (10 μM), and (e) 1 h following 100 ng/ml LPS with allopurinol addition (10 μM), after which cells were stained with 10 μM DHR123 for 30 min at 37°C. Bars=20 μm . (B) ROS amounts in LPS-treated RAW 264.7 cells as measured by DCH fluorescence. The FL1-H fluorescence intensity, represented by mean values, on a FACScan flow cytometer was elevated on LPS treatment (100 ng/ml) for 30 min. Antioxidants added prior to LPS treatment reduced the intracellular hydrogen peroxide amounts.

group or no free hydroxyl group in their chemical structure. This suggests that the radical-scavenging effects of phenylpropanoids are correlated with the number of hydroxyl groups. A similar correlation was also reported for flavonoids [23] and phenolic acid derivatives [24]. Siquet et al. reported that trihydroxycinnamic acid was more potent as an antioxidative agent compared to dihydroxycinnamic acid [25]. Lorenz et al. investigated the antioxidant and radical-scavenging activities of polyphenolic isochromans. To assess the relationship between structure and scavenging properties, hydroxyisochroman was compared with synthesized derivatives that differed in their degree of hydroxylation by substitution with methoxy groups. The scavenging capacity was higher for hydroxyisochroman bearing OH groups than the methoxy-substituted derivatives [26]. Methoxy-substituted ferulic acid, isoferulic acid, also exhibited lower effectiveness in scavenging radicals compared to caffeic acid. We suggest that the resonance structures of the radicals derived from CAPE and caffeic acid are especially stable because of the *o*-quinone form of the resonance structure. There are more resonance structures in caffeic acid and CAPE than in ferulic acid, isoferulic acid, and coumaric acids.

The crystalline structure of XO was first reported by Enroth et al. [6]. Okamoto et al. presented the crystalline structure of XO during catalysis and disclosed the catalytic mechanism of substrate hydroxylation at the active site via Mo-O-C bond formation. We employed 3D molecular docking of selected phenylpropanoids with XO to correlate with our enzyme kinetic experiments. We showed that molecular docking figures of various flavonoids bind to the active site of XO [27]. Hydroxyl groups at C5, C7, C4, and the carbonyl group of flavonoids contributed favorable hydrogen bonds and electrostatic interactions with Arg 880, Glu 1261, and Thr 1010 of XO, respectively. A hydrophobic pocket surrounded by Phe 649, Phe 1013, Phe 1076, Leu 648, Leu 873, and Leu 1014 is critical for stabilizing the phenyl group of flavonoids. Okamoto et al. reported a cocrystalline structure of an extremely potent inhibitor, TEI-6720, and XO. TEI-6720 binds in a long narrow channel leading to the active site. The amino side chain of Leu 648, Phe 649, Val 1011, and Phe 1013 in the narrow channel with distances of 3.7–4.2 Å provides a hydrophobic environment for TEI-6720 to bind with XO [28]. A similar conclusion was reported for a newly synthesized XO inhibitor, Y-700 [29]. This hydrophobic channel was the same as the hydrophobic pocket we previously disclosed which accommodates the bulky hydrophobic moiety of good inhibitors. Blocking the channel by the inhibitors prevents substrate entrance toward the Mo-pt center. In our enzyme kinetic assay experiments, we found that CAPE was a more potent inhibitor than caffeic acid. The only difference between these two compounds is that CAPE is the phenethyl ester of caffeic acid. Results of the molecular docking experiments showed that the binding motifs of both inhibitors toward XO were exactly the same, but the phenethyl group of CAPE stretched into the hydrophobic pocket provided by the amino acid residues of Phe 1076, Phe 649, Leu 648, Leu 873, and Leu 1014. We speculated that additional hydrophobic stabilization occurred due to the hydrophobic pocket of XO and the phenethyl group of CAPE. Because caffeic acid lacks this

extra stabilization, it exhibited lower inhibition potency toward XO.

The chemical structures of both caffeic acid and CAPE contain two hydroxyl groups on the benzene moiety, and these two compounds were more effective in scavenging radicals than other selected compounds, and they were also the most potent inhibitors against XO. From our molecular docking experiments, we realized that both caffeic acid and CAPE interacted favorably with the active site of XO through the formation of a hydrogen bond and electrostatic interactions between the two hydroxyl groups of the inhibitors with side chain residues of the amino acids Arg 880, Glu 1261, and Thr 1010 of XO. The chemical structure of ferulic acid is similar to that of caffeic acid with the only difference being a methoxy substituted for a hydroxyl, and this modification of the chemical structure results in diminished inhibition potency of ferulic acid against XO. This further implies that the H atom of the R2 hydroxyl plays a more important role than the O atom. When comparing the H atom of the R1 hydroxyl with the O atom, it was found to be vital for binding because *p*-methoxycinnamic acid was much less active than *p*-coumaric acid in binding to XO.

The phenylpropanoid derivatives tested herein are potent ROS scavengers, and they also are effective inhibitors against XO's reduction of ROS production. Intracellular ROS production is associated with a number of cellular events including the activation of NAD(P)H oxidase, XO, and the cellular mitochondrial respiratory chain [30]. ROS thus formed are potent activators of inflammatory signal transduction pathways, such as the MAPK cascade, which triggers a series of responses in which I κ B is phosphorylated to free NF- κ B from I κ B inhibition [31]. The active form of NF- κ B is translocated from the cytoplasm to the nucleus to bind the cognate NF- κ B binding site in the promoter regions of genes including COX-2 and iNOS [32]. CAPE with its potent antioxidant actions may suppress NF- κ B activation, and lead to suppression of iNOS and COX-2 expressions. In the *in vitro* experiment, caffeic acid was the most potent agent inhibiting XO activity and scavenging ROS (Table 4). In contrast, CAPE exhibited more potent effects in reducing ROS-associated NO production than other reference compounds in macrophage cells. It can be implied that the phenethyl ester of CAPE plays an important role in cell membrane permeability. Because there are numerous ROS sources in addition to XO, CAPE inhibits not only XO, but can also block NAD(P)H oxidase and maintain mitochondrial function to reduce ROS amounts, whereas allopurinol, ascorbate, and aminoguanidine have only a single role each of XO inhibition, ROS scavenging, and NOS inhibition, respectively.

We further confirmed that CAPE possesses greater protective activity from ROS-associated damage in β -amyloid peptide (A β)-treated neuronal cells. Even though the mechanism for A β -induced cell death is complicated, it is at least in part closely correlated with intracellular oxidative stress which causes the peroxidation of membrane lipids and ultimately leads to cell death [33]. We further evaluated the rescue effects of phenylpropanoids on Neuro 2A cells under oxidative stress. Neuro 2A cells were treated with A β_{25-35} (15 μ M) for 48 h in the presence or absence of phenylpropanoids, and the protective

effects were calculated according to the reduced cytotoxicity with phenylpropanoid treatments (1.0 μ M). CAPE was more potent than other phenylpropanoids with 50.3% protection at a concentration of 1.0 μ M. The order of the protective effects for the tested phenylpropanoids was CAPE > caffeic acid > ferulic acid > cinnamic acid (Supplemental Fig. 3A). As shown in supplemental Fig. 3B, A β -treated Neuro 2A cells (b) resulted in an increase in DHR123 fluorescence over that of the untreated control (a), while reduced fluorescence intensity was seen with the cotreatment of A β and CAPE (c). These results demonstrate that CAPE was more effective in reducing the A β -induced rise in ROS levels. Our experimental findings should be beneficial in medicinal applications to ROS-associated diseases.

Acknowledgments

This study was supported by a grant (NSC95-2113-M-038-002) from the National Science Council and by a Topnotch Stroke Research Center Grant, Ministry of Education.

Appendix A. Supplementary data

Supplementary data associated with this article can be found, in the online version, at doi:10.1016/j.freeradbiomed.2007.08.018.

References

- [1] Cuzzocrea, S.; Riley, D. P.; Caputi, A. P.; Salvemini, D. Antioxidant therapy: a new pharmacological approach in shock, inflammation, and ischemia/reperfusion injury. *Pharmacol. Rev.* **53**:135–159; 2001.
- [2] Nakai, K.; Kadiiska, M. B.; Jiang, J. J.; Stadler, K.; Mason, R. P. Free radical production requires both inducible nitric oxide synthase and xanthine oxidase in LPS-treated skin. *Proc. Natl. Acad. Sci. USA* **103**:4616–4621; 2006.
- [3] Schroder, K.; Vecchione, C.; Jung, O.; Schreiber, J. G.; Shiri-Sverdlov, R.; van Gorp, P. J.; Busse, R.; Brandes, R. P. Xanthine oxidase inhibitor tungsten prevents the development of atherosclerosis in ApoE knockout mice fed a Western-type diet. *Free Radic. Biol. Med.* **41**:1353–1360; 2006.
- [4] Okamoto, K.; Matsumoto, K.; Hille, R.; Eger, B. T.; Pai, E. F.; Nishino, T. The crystal structure of xanthine oxidoreductase during catalysis: implications for reaction mechanism and enzyme inhibition. *Proc. Natl. Acad. Sci. USA* **101**:7931–7936; 2004.
- [5] Olson, J. S.; Ballou, D. P.; Palmer, G.; Massey, V. The mechanism of action of xanthine oxidase. *J. Biol. Chem.* **249**:4363–4382; 1974.
- [6] Enroth, C.; Eger, B. T.; Okamoto, K.; Nishino, T.; Nishino, T.; Pai, E. F. Crystal structures of bovine milk xanthine dehydrogenase and xanthine oxidase: structure-based mechanism of conversion. *Proc. Natl. Acad. Sci. USA* **97**:10723–10728; 2000.
- [7] Bravo, L. Polyphenols: chemistry, dietary sources, metabolism, and nutritional significance. *Nutr. Rev.* **56**:317–333; 1998.
- [8] Chan, W. S.; Wen, P. C.; Chiang, H. C. Structure-activity relationship of caffeic acid analogues on xanthine oxidase inhibition. *Anticancer Res.* **15**:703–707; 1995.
- [9] Ermilov, A.; Diamond, M. P.; Sacco, A. G.; Dozortsev, D. D. Culture media and their components differ in their ability to scavenge reactive oxygen species in the plasmid relaxation assay. *Fertil. Steril.* **72**:154–157; 1999.
- [10] Chen, C.; Tang, H. R.; Sutcliffe, L. H.; Belton, P. S. Green tea polyphenols react with 1,1-diphenyl-2-picrylhydrazyl free radicals in the bilayer of liposomes: direct evidence from electron spin resonance studies. *J. Agric. Food Chem.* **48**:5710–5714; 2000.
- [11] Lin, C. M.; Chen, C. T.; Lee, H. H.; Lin, J. K. Prevention of cellular ROS damage by isovitexin and related flavonoids. *Planta Med.* **68**:365–367; 2002.
- [12] Morris, G. M.; Goodsell, D. S.; Halliday, R. S.; Huey, R.; Hart, W. E.; Belew, R. K.; Olson, A. J. Automated docking using a Lamarckian genetic algorithm and empirical binding free energy function. *J. Comput. Chem.* **19**:1639–1662; 1998.
- [13] Gasteiger, J.; Marsili, M. Iterative partial equalization of orbital electro-negativity—a rapid access to atomic charges. *Tetrahedron* **36**:3219–3228; 1980.
- [14] Lin, C. M.; Huang, S. T.; Lee, F. W.; Kuo, H. S.; Lin, M. H. 6-Acyl-4-aryl/alkyl-5,7-dihydroxy-coumarins as anti-inflammatory agents. *Bioorg. Med. Chem.* **14**:4402–4409; 2006.
- [15] Kurihara, H.; Fukami, H.; Toyoda, Y.; Kageyama, N.; Tsuruoka, N.; Shibata, H.; Kiso, Y.; Tanaka, T. Inhibitory effect of oolong tea on the oxidative state of low density lipoprotein (LDL). *Biol. Pharm. Bull.* **26**:739–742; 2003.
- [16] Kim, H.; Lee, H. S.; Chang, K. T.; Ko, T. H.; Baek, K. J.; Kwon, N. S. Chloromethyl ketones block induction of nitric oxide synthase in murine macrophages by preventing activation of nuclear factor-kappa B. *J. Immunol.* **154**:4741–4748; 1995.
- [17] Keller, J. N.; Guo, Q.; Holtsberg, F. W.; Bruce-Keller, A. J.; Mattson, M. P. Increased sensitivity to mitochondrial toxin-induced apoptosis in neural cells expressing mutant presenilin-1 is linked to perturbed calcium homeostasis and enhanced oxyradical production. *J. Neurosci.* **18**:4439–4450; 1998.
- [18] Ubezio, P.; Civoli, F. Flow cytometric detection of hydrogen peroxide production induced by doxorubicin in cancer cells. *Free Radic. Biol. Med.* **16**:509–516; 1994.
- [19] Kikuzaki, H.; Hisamoto, M.; Hirose, K.; Akiyama, K.; Taniguchi, H. Antioxidant properties of ferulic acid and its related compounds. *J. Agric. Food Chem.* **50**:2161–2168; 2002.
- [20] Krizkova, L.; Nagy, M.; Polonyi, J.; Dobias, J.; Belicova, A.; Grancai, D.; Krajcovic, J. Phenolic acids inhibit chloroplast mutagenesis in *Euglena gracilis*. *Mutat. Res.* **469**:107–114; 2000.
- [21] Kampa, M.; Alexaki, V. I.; Notas, G.; Nifli, A. P.; Nistikaki, A.; Hatzoglou, A.; Bakogeorgou, E.; Kouimtzooglou, E.; Blekas, G.; Boskou, D.; Gravanis, A.; Castanas, E. Antiproliferative and apoptotic effects of selective phenolic acids on T47D human breast cancer cells: potential mechanisms of action. *Breast Cancer Res.* **6**:R63–R74; 2004.
- [22] Ilhan, A.; Akyol, O.; Gurel, A.; Armutcu, F.; Iraz, M.; Oztas, E. Protective effects of caffeic acid phenethyl ester against experimental allergic encephalomyelitis-induced oxidative stress in rats. *Free Radic. Biol. Med.* **37**:386–394; 2004.
- [23] Heim, K. E.; Tagliaferro, A. R.; Bobilya, D. J. Flavonoid antioxidants: chemistry, metabolism and structure-activity relationships. *J. Nutr. Biochem.* **13**:572–584; 2002.
- [24] Silva, F. A.; Borges, F.; Ferreira, M. A. Effects of phenolic propyl esters on the oxidative stability of refined sunflower oil. *J. Agric. Food Chem.* **49**:3936–3941; 2001.
- [25] Siquet, C.; Paiva-Martins, F.; Lima, J. L.; Reis, S.; Borges, F. Antioxidant profile of dihydroxy- and trihydroxyphenolic acids—a structure-activity relationship study. *Free Radic. Res.* **40**:433–442; 2006.
- [26] Lorenz, P.; Zeh, M.; Martens-Lobenhoffer, J.; Schmidt, H.; Wolf, G.; Horn, T. F. Natural and newly synthesized hydroxy-1-aryl-isochromans: a class of potential antioxidants and radical scavengers. *Free Radic. Res.* **39**:535–545; 2005.
- [27] Lin, C. M.; Chen, C. S.; Chen, C. T.; Liang, Y. C.; Lin, J. K. Molecular modeling of flavonoids that inhibits xanthine oxidase. *Biochem. Biophys. Res. Commun.* **294**:167–172; 2002.
- [28] Okamoto, K.; Eger, B. T.; Nishino, T.; Kondo, S.; Pai, E. F.; Nishino, T. An extremely potent inhibitor of xanthine oxidoreductase. Crystal structure of the enzyme-inhibitor complex and mechanism of inhibition. *J. Biol. Chem.* **278**:1848–1855; 2003.
- [29] Fukunari, A.; Okamoto, K.; Nishino, T.; Eger, B. T.; Pai, E. F.; Kamezawa, M.; Yamada, I.; Kato, N. Y-700 [1-[3-cyano-4-(2,2-dimethylpropoxy)phenyl]-1H-pyrazole-4-carboxylic acid]: a potent xanthine oxidoreductase inhibitor with hepatic excretion. *J. Pharmacol. Exp. Ther.* **311**:519–528; 2004.

- [30] Abramov, A. Y.; Scorziello, A.; Duchen, M. R. Three distinct mechanisms generate oxygen free radicals in neurons and contribute to cell death during anoxia and reoxygenation. *J. Neurosci.* **27**:1129–1138; 2007.
- [31] Choi, H. B.; Ryu, J. K.; Kim, S. U.; McLarnon, J. G. Modulation of the purinergic P2X7 receptor attenuates lipopolysaccharide-mediated microglial activation and neuronal damage in inflamed brain. *J. Neurosci.* **27**: 4957–4968; 2007.
- [32] Chun, K. S.; Cha, H. H.; Shin, J. W.; Na, H. K.; Park, K. K.; Chung, W. Y.; Surh, Y. J. Nitric oxide induces expression of cyclooxygenase-2 in mouse skin through activation of NF-kappaB. *Carcinogenesis* **25**:445–454; 2004.
- [33] Longpre, F.; Garneau, P.; Christen, Y.; Ramassamy, C. Protection by EGb 761 against beta-amyloid-induced neurotoxicity: involvement of NF-kappaB, SIRT1, and MAPKs pathways and inhibition of amyloid fibril formation. *Free Radic. Biol. Med.* **41**:1781–1794; 2006.